JMEPEG (2009) 18:672–678
DOI: 10.1007/s11665-009-9417-7

1059-9495/$19.00

Carbon Fiber-Reinforced Smart Laminates with Embedded SMA Actuators—Part II: Numerical Models and Empirical Correlations

M. Riva, P. Bettini, L. Di Landro, G. Sala, and A. Airoldi

(Submitted October 21, 2008; in revised form February 16, 2009)

Up to now one of the main limitations for a large use of shape memory alloys (SMA)-based smart composite structures in the aerospace industry is the lack of useful numerical tools for design; in addition, some technological aspects still need a more detailed investigation. This article shows numerical modeling approaches adopted for the implementation of SMA constitutive laws in commercial codes such as ABAQUS. Two different approaches were selected. The first one is based on the thermomechanical model proposed by Turner and the other one follows the thermodynamic macromechanical constitutive law developed by Lagoudas. The implementation in ABAQUS code was followed by a procedure to evaluate model parameters and to experimentally validate the reliability of code predictions for specifically designed test situations. This article presents the test campaign carried out for the definition of these parameters and the numerical-experimental correlation for both the models.

Keywords embedded SMA, polymer matrix composites, shape memory alloy, smart structures

1. Introduction

Materials for primary structures in aerospace applications must have high mechanical properties, lightness, and durability. It is important for these structures to exhibit good behavior particularly in terms of impact resistance and environmental endurance; fire and corrosion resistance are further characteristics often required. Composite materials often conform well to such requirements and nowadays are widely used in many engineering fields.

On the other hand, a number of new materials and technologies (i.e., microelectronic devices, shape memory alloys (SMA)-based microactuators, piezo-ceramics, electroactive polymers, optical fibers, etc.) allow to realize structures able to actively respond to specific external inputs. Thus, extensive diffusion of smart materials in many aerospace and ground commercial applications is expected. Their capabilities in terms of shape and vibration control of large space structures, acoustic control for noise reduction in civil aircraft, health monitoring, and in-site structure identification are well assessed and promising results are also obtained in many other applications.

In the last years, several research activities in the manufacturing processes field were devoted to develop smart structures that could combine high mechanical efficiency, due to composite host materials, with good functional properties of embedded sensors and actuators (Ref 1-3).

The embedding of these smart devices into the structures could give some advantages compared to their bonding onto the outer skin. For example, they allow the actuation in locations hardly accessible from outside because of shape constraints; the protection of the actuation system inside the host structure from all environmental effects reducing its performance can be also achieved; in addition, active structures could be applied even in those cases where a clean surface is required (i.e., skin of the aerodynamic surfaces) (Ref 4).

The embedding technique of these components within the load-carrying structure is still a leading-edge application. Moreover, research activities must be oriented both to the development of those manufacturing techniques and to the characterization of embedded sensors and actuators invasivity (active and passive) on the smart structure performance.

This article is an invited paper selected from presentations at Shape Memory and Superelastic Technologies 2008, held September 21-25, 2008, in Stresa, Italy, and has been expanded from the original presentation.

M. Riva, P. Bettini, L. Di Landro, G. Sala and **A. Airoldi**, Aerospace Engineering Department, Politecnico di Milano, Milan, Italy. Contact e-mail: riva@aero.polimi.it.

Nomenclature

A_s, A_f	austenite start and finish temperature
CTE	coefficient of thermal expansion
CFRSL	carbon fiber-reinforced smart laminates
FE	finite element
M_s, M_f	martensite start and finish temperature
OWSME	one-way shape memory effect
SMA	shape memory alloys
TWSME	two-way shape memory effect
T_g	glass transition temperature

Finally, most of the applications are also strongly dependent on the availability of useful numerical tools. In fact, all the design activities regarding structures are nowadays related to the adoption of numerical models able to predict the efficiency and performance of the systems (Ref 5). The peculiarity of smart composite structures underlines this problem due to the higher complexity of the active materials behavior: the typically nonlinear response of these materials joined to the composite material modeling, which must account for laminates anisotropy and complex damage mechanism pose a difficult task.

In view of a development of both technological processes and numerical tools for smart carbon laminates with embedded sensors and actuators, this research is focused on the embedding of shape memory wires, selectively taking advantage of their functional properties in terms of low activation speed combined with high authority, i.e., capacity to effectively transfer their load/deformation to the host structure. In fact, these characteristics are useful for most of the aerospace applications (airfoil morphing, shape control, etc.). Authority of these actuators can be exploited in two different ways. First, the wires are embedded in a detwinned martensite phase and the activation of the structure is obtained using the OWSME due to the reverse transition induced by heating (from detwinned martensite to the austenite phase); then the structure (and the embedded wires too) come back to the initial form through its stiffness (host material remain in the elastic range) when the wires are cooled and the forward transition is induced. Second, the wires can be embedded both in austenite or detwinned martensite phase considering TWSME. A structure can change its form by heating or cooling so that reverse or forward transition, respectively, occurs (Ref 6, 7).

A previous work was oriented to the description of the embedding techniques developed for SMA actuators and the analysis of the interface with the host materials (Ref 8). This article is focused on numerical aspects. The target is the definition of a design strategy that takes into account the computational cost and the level of accuracy required by a smart structure for a preliminary prediction of the overall performance of the system. The implementation of the constitutive laws of the actuators in commercial codes is the crucial point for the modeling of several actuators and is still an open issue regarding shape memory actuators. Several constitutive laws have been developed in the last decade for the prediction of the behavior of SMAs. These laws derive from micromechanical approaches (Ref 5) or are based on macromechanical models (Ref 9-14). Liang and Rogers (Ref 9) or Turner (Ref 12, 14) proposed a description of material behavior on a phenomenological basis; Tanaka and Lagoudas (Ref 10, 11) proposed a constitutive law based on thermodynamical approaches. This work is focused on the implementation and comparison between the relatively simple model (Ref 12, 14) with the more detailed one (Ref 11) to have two different tools depending on the accuracy required by the application design.

2. Design and Modeling of Smart Structure

Smart structures design is strongly dependent on the availability of useful numerical tools for the performance prediction of the whole system. In this article, the attention is focused on two complementary constitutive laws: the first one is the Lagoudas' thermodynamical model and the other is the Turner's thermomechanical model. The work was oriented to implement these constitutive laws in ABAQUS, a commercial code, trying to identify the peculiarity of the two different models to have a criterium for the proper numerical procedure selection.

The finite element analysis time, considered as the sum of the time required to prepare the FE model and the solving time, played an important role in the choice of a modeling technique. The capabilities of the constitutive laws were also taken into account in terms of how well they represent of the real behavior of the modeled SMA (two way shape memory effect, superelasticity, hysteresis modeling, etc.).

2.1 Turner Model

The Turner model assumes a nonlinear thermoelastic behavior defining an effective coefficient of thermal expansion (CTE) starting from the classic total strain definition. The strain applied to a SMA is the sum of mechanical, thermal, and transformation contributes:

$$\varepsilon = \varepsilon_e + \varepsilon_p + \varepsilon_{th} + \varepsilon_m \qquad \text{(Eq 1)}$$

where ε_e, ε_p, and ε_{th} are the elastic, plastic, and thermal strains, respectively and ε_m derives from the phase transition. Considering the loading situations below the elastic limit, the plastic deformation can be dismissed. The elastic strain can be expressed as the ratio between applied stress and a temperature-dependent Young modulus. An equivalent thermal strain $\tilde{\varepsilon}_{th}$ can be introduced that encompasses both transition induced and thermal strains. The model considers that this factor is equal to the simple thermal strain of martensite phase when the temperature is less or equal to A_S. When the temperature exceeds this value, another thermal contribution is introduced, which depends on a temperature-dependent fictitious expansion coefficient CTE $\alpha_E(T)$. This can be written as:

$$\tilde{\varepsilon}_{th} = \begin{cases} \alpha_M(T - T_0) & T \le A_S \\ \alpha_M(T - T_0) + \alpha_E(T)(T - A_S) & T > A_S \end{cases} \qquad \text{(Eq 2)}$$

By writing Eq 2 ($T > A_S$) in an explicit form with respect to the effective CTE, one obtains:

$$\alpha_E(T) = \frac{\tilde{\varepsilon}_{th} + \alpha_M(T_0 - A_S)}{T - A_S} \quad \text{with} \quad \tilde{\varepsilon}_{th} = \frac{\sigma_{REC}(T)}{E(T)} \qquad \text{(Eq 3)}$$

The $\sigma_{REC}(T)$ is the recovery stress function dependent on temperature. All the parameters can be determined with empirical tests. In fact α_M and A_S are obtained from dilatometric and calorimetric tests (dilatometer and differential scanning calorimeter). Then, $E(T)$ and $\sigma_{REC}(T)$ can be measured through tensile tests at different temperatures (isothermal) (Fig. 1) and constrained activation tests (isolength), respectively. Considering the characteristics of Turner model, it is apparent that this is able to model the recovery phase of OWSME only.

The implementation in commercial codes, like ABAQUS, is quite simple because the software allows the definition of temperature-dependent material properties and, in particular, Young modulus ($E(T)$, Fig. 1) and CTE ($\alpha_E(T)$, Fig. 2). A thermal analysis is performed (temperature is the only degree of freedom) to define the temperature map for each step. This thermal field is then applied to the complete model to define the strain displacement and the stress fields.

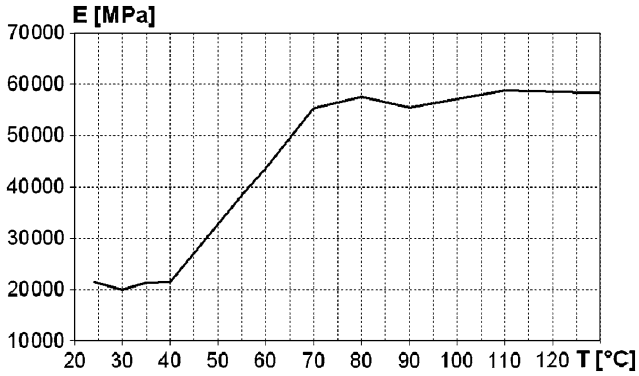

Fig. 1 NiTiNol temperature-dependent Young Modulus

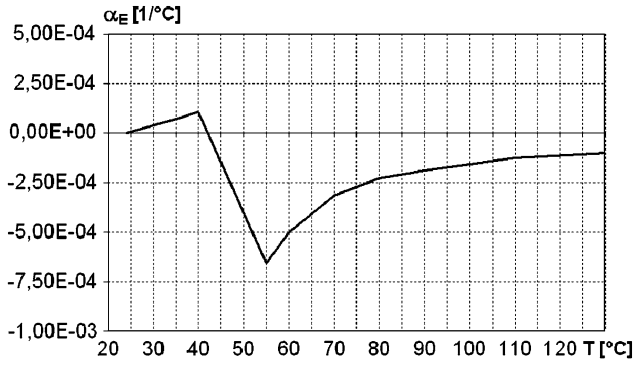

Fig. 2 NiTiNol temperature-dependent CTE

2.2 Lagoudas Model

The Lagoudas model was implemented in a reduced formulation; to take advantage of the actuators shape (wires), it was simplified into a one-dimensional law. The plastic deformation was neglected following the similar reduction imposed in the Turner model. The model is based on five state variables: strain ε, stress σ, temperature T, martensitic fraction ξ, and martensitic strain ε_m.

The constitutive equations are:

$$\begin{aligned}\varepsilon &= S\sigma + \alpha(T - T_0) + \varepsilon_m \\ S &= \frac{1}{E^A} + \xi\left(\frac{1}{E^M} - \frac{1}{E^A}\right) \\ \alpha &= \alpha^A + \xi(\alpha^M - \alpha^A)\end{aligned} \quad \text{(Eq 4)}$$

where S is the compliance, α is the CTE, and T_0 is the reference environment temperature; according to Lagoudas model, the evolution of the martensitic transformation is considered similar to a plastic deformation and defines the flow rule in its differential form (Ref 11, 13)

$$\dot{\varepsilon}_m = \Lambda\dot{\xi} \quad \text{where} \quad \Lambda = \begin{cases} H^{cur}\text{sign}\left(\Sigma^{eff}\right), & \dot{\xi} > 0 \\ \frac{\varepsilon^m_{max}}{\xi_{max}}, & \dot{\xi} < 0 \end{cases} \quad \text{(Eq 5)}$$

In this formulation, Λ is the transformation tensor, the expressions $\dot{\xi} > 0$ and $\dot{\xi} < 0$ specify the transition phase direction, H^{cur} is the current maximum deformation strain (dependent on the applied stress), Σ^{eff} is the effective stress, ε^m_{max} is the maximal martensite strain ever reached in the process, and ξ_{max} is the correspondent martensitic fraction. Lagoudas defines an empirical formula (Ref 11, 13) for the definition of the Σ^{eff} that is, in fact, the stress that causes the phase transition and depends on the martensitic fraction, the deformation, and some material parameters:

$$\Sigma^{eff} = \sigma + \left\{-D_3\left[-\ln\left(1 - \xi^d\right)\right]^{\frac{1}{m_1}} + D_2 H \xi^d + D_1\right\}\text{sign}(\varepsilon_m)$$

The strain evolution consequent to the martensitic fraction is treated as a plastic deformation, and a function Φ that determines the behavior of the transition is defined as follows:

$$\Phi \le 0, \quad \Phi\dot{\xi} = 0, \quad \Phi = \begin{cases} \Pi - Y, & \dot{\xi} > 0 \\ -\Pi - Y, & \dot{\xi} < 0 \end{cases} \quad \text{(Eq 6)}$$

where Y is a material constant, which defines the energy dissipation over volume due to a complete transformation. Π is the thermodynamic force which drives the transformations and is representative of the chance that this phenomenon is occurring. It is experimentally defined by a function dependent on characteristic temperatures of the material and other material parameters.

$$\begin{aligned}\Pi = \Sigma^{eff}\Lambda + \frac{1}{2}\Delta S\sigma^2 + \sigma\Delta\alpha(T - T_0) + \rho\Delta s_0(T - M^{0S}) + D_4\xi \\ - \rho\Delta c\left[T - T_0 - T\ln\left(\frac{T}{T_0}\right)\right] - D_5[-\ln(1 - \xi)]^{\frac{1}{m_2}} + Y\end{aligned}$$

The finite element method implies the solving of the nonlinear system $[K(\{u\})]\{u\} = \{F\}$, where the nonlinearity is due to the dependence of the stiffness matrix ($\{K\}$) on the displacement variable $\{u\}$ and $\{F\}$ is the loading vector. The implementation into the ABAQUS code of this model was done writing a UMAT (User Material) subroutine, which allows the user to define the material behavior. UMAT initializes the state variables with a function called SDVINI (Solution-Dependent INItial Variables) and then evaluates them in each time increment using the Lagoudas formulation. The state variables (σ, ε, T, ξ, ε^m) are managed by the STATEV (STATE Variables) parameter that interacts between the subroutine and the main code. A return mapping closest point projection algorithm was adopted for the evaluation of strains and temperatures at each step, which verifies if the transition phase is occurring (Ref 15, 16). The subroutine extracts the state variables from ABAQUS and by applying mechanical or thermal strains, it derives the new stress and the transition function Φ; if the transition is not occurring, the prediction is accepted and the state variables are updated for the next step, otherwise, if the transition is in process, the subroutine considers substeps where imposed strains and temperatures are fixed and a variation of ξ and ε^m is applied to evaluate the transition tensor and the influence of the transition phase on the state variables for this step.

2.2.1 Constitutive Law Calibration. To model the NiTiNOL wires, a subroutine was developed taking into account the unidimensional simplified model. This choice also simplifies the calibration of the subroutine because starting from the Lagoudas formulation there are 19 parameters to be obtained through proper experimental measurements. These are listed in Table 1.

Most of these parameters can, in principle, be obtained through thermomechanical tests, whereas back-and-drag-stress-related parameters are obtained by interpolation on the basis of specific experimental tests.

2.3 Comparisons

A useful numerical approach should be flexible and easy to implement, but, at the same time, it has to significantly represent the smart structures. The constitutive models considered here are in this sense complementary. The Turner model is characterized by easy implementation and low CPU time, but it is not able to adequately describe the transition from detwinned martensite to austenite; moreover, it does not take into account the "hysteresis" between the two transitions (back and forward). On the other hand, the Lagoudas law is able to cover those deficiencies, but it requires too long solving time to be used in a design and optimization phase.

In this research, both models were applied. Usually, the procedure implemented requires a preliminary modeling using the faster Turner model to allow operations like optimization and performances prediction. The following step, when necessary, consists in the implementation of the Lagoudas model to have a more detailed description of the performances particularly in terms of deployable load, back and forward transition, and phase transitions.

Table 1 Lagoudas parameters

Martensitic and austenitic physical constants	
E^A,E^M	Young's moduli
ν^A,ν^M	Poisson coefficients
α^A,α^M	Thermal expansion coefficients
ρc^A,ρc^M	Specific heats
$\rho\Delta s^0$	Specific enthalpy difference
Transition phase parameters	
H	Maximum transition strain
Y	Total hysteresis for a single transition cycle
M^{0S}	Starting martensite temperature
D_1, D_2, D_3, m_1	Back stress-related parameters
D_4, D_5, m_2	Drag stress-related parameters

3. Experimental Validation

The two models were validated by testing dedicated specimens specifically manufactured. The Turner model was used for the experimental/numerical comparison with a carbon fiber-reinforced panel with OWSME NiTiNOL wires embedded, whereas the Lagoudas model was validated with a simple wire of both OWSME and TWSME (Ref 21). NiTiNOL wires from Furukawa Techno Materials with diameter of 0.38 mm were employed.

3.1 Turner Model Validation

Different verification models were performed to select the type of the elements. The comparison underlines how a shell model is precise enough with a high gain in terms of CPU time. Due to this consideration, the final comparison was conducted on a shell-based model, which contains NiTiNOL wires, modeled via proper ABAQUS properties: REBAR consisting in the modeling of a reinforcing inclusion made by a proper material in a shell element (Fig. 3). The thermoelastic model receives as input the thermal load on the wires and derives the temperature behavior of all the nodes.

A carbon fiber-reinforced panel with two embedded NiTiNOL wires was modeled and analyzed using the ABAQUS commercial code. The actual panel was manufactured with 12 plies $[90°/(0°)_2/90°/+45°/-45°]_s$ and its overall dimensions were: $30 \times 170 \times 1.2$ mm. The actuators chosen were OWSME wires ($\varnothing$ = 0.38 mm) trained using standard heat treatments in accordance with Ref 17. They were embedded between the 2nd and 3rd plies with a 4% imposed strain. All manufacturing techniques and mechanical characteristics are reported in Ref 8. The panel was constrained on one side and it was activated via Joule effect (Fig. 4). The numerical/experimental comparison shows that, after a short transition, the predicted displacement matches (max. error 20 μm) the experimental one (Fig. 5).

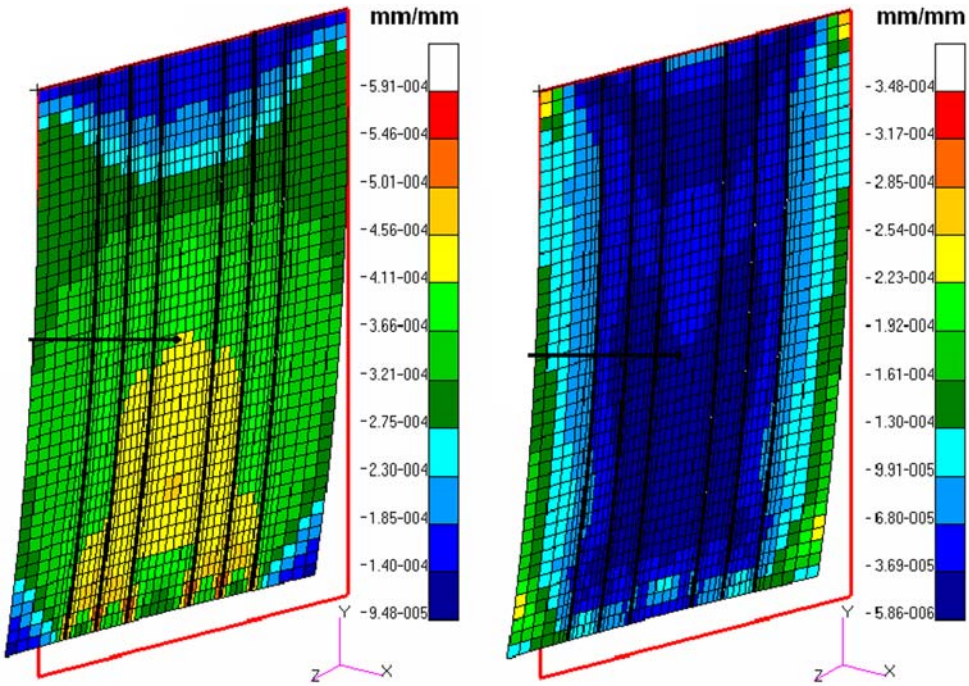

Fig. 3 FE model of the Turner experiment

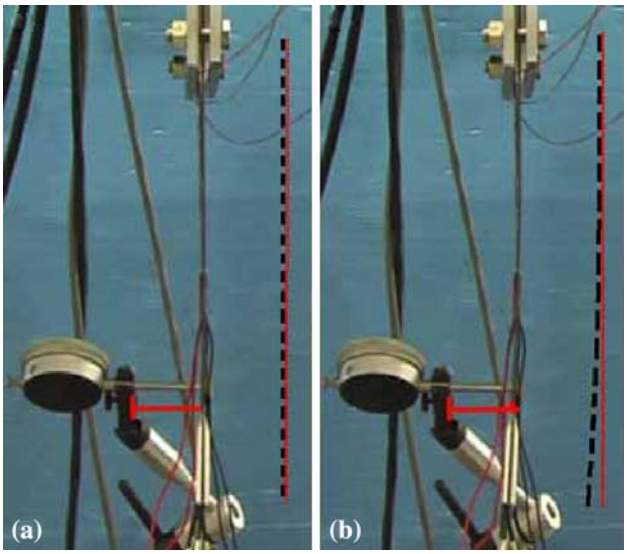

Fig. 4 Turner validation experimental test setup

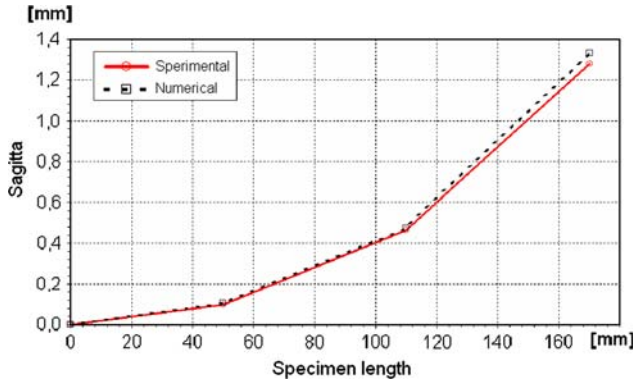

Fig. 5 FE displacement comparison for the Turner model

3.2 Lagoudas Validation

The validation model is very simple; in fact, it was decided to adopt a single ABAQUS TRUSS element, which has two nodes and two linear degrees of freedom per node, to reduce the elevated analysis time due to the subroutine implementation. One of the nodes was constrained keeping the other free. For the applied stress cases, a *DLOAD card was used, which applies axial stress to the element along its main direction. The thermal load was applied in two steps: a cooling down from 393.15 to 273.15 K and a heating to the initial temperature. The first validation was conducted on the Lagoudas experimental test by considering the calibration parameters presented in Ref 11.

The experiment selected for the validation of the subroutine was a simple DMA tensile test. The specimen is heated up to a temperature higher than its A_f and cooled down below the M_f. One tip of the wire is constrained while the other is fixed on a movable part, which is able to induce a constant stress (at a desired level) during the whole test. The strain is recorded and plotted with respect to the temperature, obtaining the typical behavior of Fig. 6. Figure 7 shows that the results derived from Lagoudas model and that implemented for the ABAQUS code

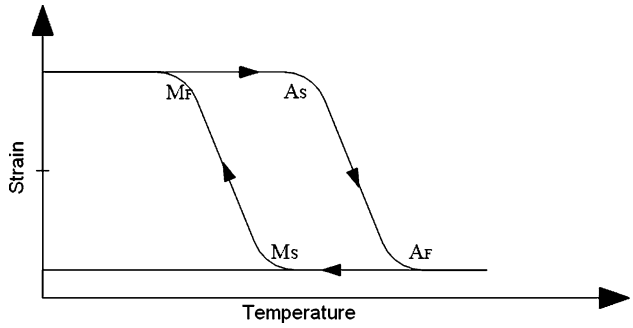

Fig. 6 Typical temperature vs. strain behavior for SMA

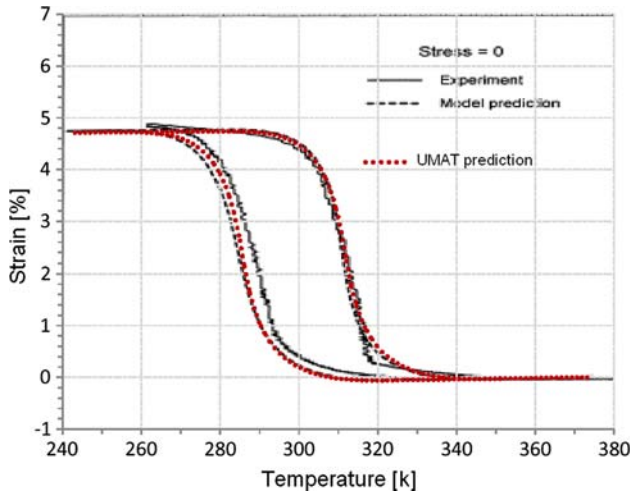

Fig. 7 Comparison between UMAT, Lagoudas, and experimental results

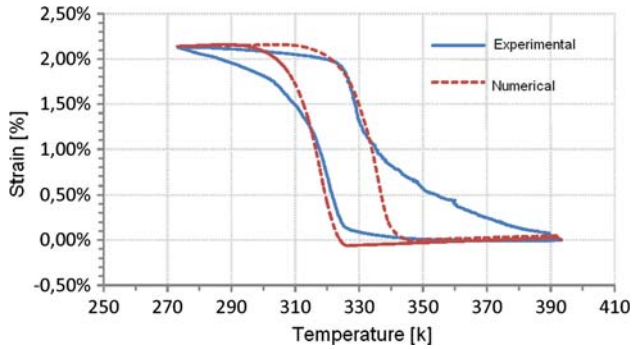

Fig. 8 Correlation of one-way trained wire with 20 MPa applied stress

are almost coincident. Both the routines follow the experimental results very well, either in terms of local predictions (i.e., transition temperatures and maximum strain) or in terms of overall predictions (general temperature and strain behavior).

The OWSME wires were experimentally tested and compared with numerical results considering a constant applied stress during the whole test. Figures 8 and 9 show an overall good correlation. In particular, it can be underlined that the starting temperatures A_s and M_s are reproduced well by the UMAT subroutine; the maximum strain is also predicted with

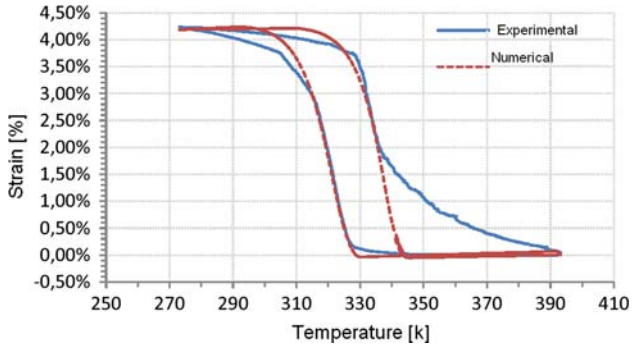

Fig. 9 Correlation of one-way trained wire with 50 MPa applied stress

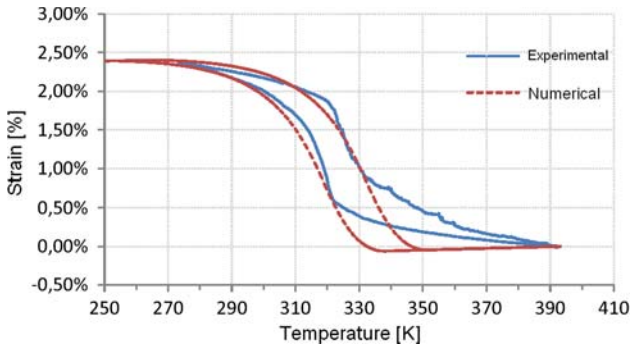

Fig. 10 Correlation of two-way trained wire without applied stress

limited error and finally the first portion of each transition (M to A and A to M) has a good correlation. Some of the mismatch (in particular the final part of the reverse transition) can be the result of previous heat treatments conducted on the same wire used as specimen.

The numerical validation of the TWSME was conducted for both the unloaded (Fig. 10) and loaded specimen tests (Fig. 11). Also in this case, the maximum strain is reproduced well. Somewhat lower agreement is presented in the transition temperatures. This could be induced by some imperfections in the two-way training process, or to the fact that the calibration of the model was done with different wires, although of the same batch, which have been subjected to several heat treatments.

4. Conclusions

The numerical tools developed can help both the performance prediction (Turner's model) and a behavior verification in terms of stress-induced transition level and characteristic temperatures (M_s, M_f, A_s, and A_f).

Considering the results derived from the two different models implemented, a modeling strategy to be applied to several smart structures was setup. Turner model is used for a preliminary performance prediction in terms of maximum displacement and stresses induced by the actuator into the structure. The lightness of this modeling technique guarantees useful optimization of the positioning procedure and dimension choice of the actuators. The Lagoudas model can be used after

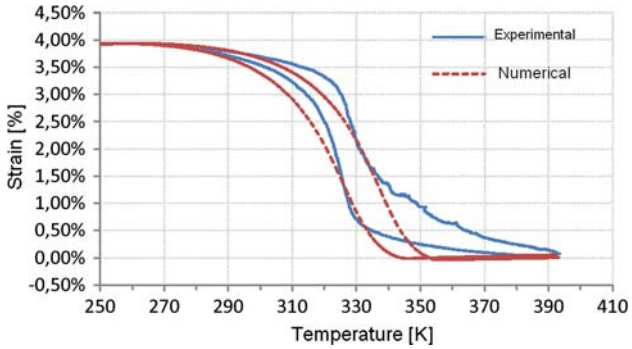

Fig. 11 Correlation of two-way trained wire with 40 MPa applied stress

the optimization process to verify the stress induced from the structure to the actuators and the consequent variation in the transition temperatures of the active materials. In this case, a further loop with Turner model, if the A_f is higher than the glass transition temperature (T_g) of the matrix, may be required.

Future work is in progress to test different host materials and types of SMA actuators. Thus, smart structures modeling and manufacturing taking advantages of the know-how acquired will move from simple specimen panels to more complex smart structures, such as laminates with single or double curvature.

Acknowledgment

The sponsorship of FIRB project RBIP06AWF9 is gratefully acknowledged.

References

1. I. Chopra, Review of State of Art Smart Structures and Integrated Systems, *AIAA J.*, 2002, **40**(11), p 2145–2187
2. S.P. Thompson and J. Loughlan, Adaptive Post Buckling Response of Carbon Fibre Plates Employing SMA Actuators, *Compos. Struct.*, 1997, **38**(1–4), p 667–678
3. Y.J. Zheng, L.S. Cui, and J. Schrooten, Basic Design Guidelines for SMA/Epoxy Smart Composites, *Mater. Sci. Eng. A*, 2005, **390**, p 139–143
4. P. Gaudenzi, M. Olivier, G. Sala, D. Sciacovelli, M. Wheelan, P. Bettini, G. Nosenzo, and A. Tralli, Development of an Active Composite with Embedded Piezoelectric Sensors and Actuators for Structure Actuation and Control, *Proceedings of the 54th International Astronautical*, IAC-03-I.4.03 (Bremen, Germany), 2003
5. Q.P. Sun and K.C. Hwang, Micromechanics Modeling for the Constitutive Behavior of Polycrystalline Shape Memory Alloys, *J. Mech. Phys. Solids*, 1993, **41**(I), p 1–17, (II), p 19–33
6. M. Cho and S. Kim, Structural Morphing Using Two-Way Shape Memory Effect of SMA, *Int. J. Solids Struct.*, 2005, **42**, p 1759–1776
7. M. Langelaar and F. van Keulen, Design Optimization of Shape Memory Alloy Structures, *10th AIAA/ISSMO Multidisciplinary Analysis and Optimization Conference* (Albany, NY)
8. P. Bettini, M. Riva, G. Sala, L. Di Landro, A. Airoldi, and J. Cucco, Carbon Fiber Reinforced Smart Laminates with Embedded SMA Actuators—Part I: Embedding Techniques & Interface Analysis, accepted in the August 2009 SMST Special Issue of *J. Mater. Eng. Perform*. doi:10.1007/s11665-009-9384-z
9. C. Liang and C.A. Rogers, One-Dimensional Thermomechanical Constitutive Relations for Shape Memory Materials, *J. Intell. Mater. Syst. Struct.*, 1990, **1**(2), p 207–234
10. K. Tanaka, F. Nishimura, T. Hayashi, H. Tobushi, and C. Lexcellent, Phenomenological Analysis on Subloops and Cyclic Behavior in Shape Memory Alloys Under Mechanical and/or Thermal Loads, *Mech. Mater.*, 1995, **19**, p 281–292

11. D.C. Lagoudas and Z. Bo, Thermomechanical Modeling of Polycrystalline SMAs Under Cyclic Loading, *Int. J. Eng. Sci.*, 1999, **37**(Part I, II, III, IV), p 1089–1204
12. T.L. Turner, 2001 "Thermomechanical Response of Shape Memory Alloy Hybrid Composites", NASA-2001-tm210656, Langley Research Center, Hampton, VA
13. D.C. Lagoudas and P.B. Entchev, Modeling of Transformation-Induced Plasticity and its Effect on the Behavior of Porous Shape Memory Alloys. Part I: Constitutive Model for Fully Dense SMAs, *Mech. Mater.*, 2004, **36**, p 865–892
14. T.L. Turner, 2001 "Experimental Validation of a Thermoelastic Model for SMA Hybrid Composites", NASA-2001-8spie-tlt24, NASA Langley Research Center, Hampton, VA
15. J.C. Simo and S. Govindjee, Non-Linear B-Stability and Symmetry Preserving Return Mapping Algorithms for Plasticity and Viscoplasticity, *Int. J. Numer. Methods Eng.*, 1991, **31**, p 151–176
16. M.A. Qidwai and D.C. Lagoudas, Numerical Implementation of Shape Memory Alloy Thermomechanical Constitutive Model Using Return Mapping Algorithms, *Int. J. Numer. Methods Eng.*, 2000, **47**, p 1123–1168
17. F. Peterson, "Method of Training NiTiNOL Wire," US Patent 6797083, 28 Sep 2004
18. T.L. Turner and H.D. Patel, "Input Files and Procedures for Analysis of SMA Hybrid Composite Beams in MSC.Nastran and ABAQUS", NASA-TM-2005-213517, NASA Langley Research Center, Hampton, VA
19. E. Patoor, D.C. Lagoudas, P.V. Entchev, L.C. Brinson, and X. Gao, Shape Memory Alloys, Part I: General Properties and Modeling of Single Crystal, *Mech. Mater.*, 2006, **38**, p 391–429
20. L. Colonna Preti, "Microattuatori in leghe a memoria di forma: sperimentazione, implementazione di leggi costitutive e validazione numerico-sperimentale", Master Thesis, Politecnico di Milano, 2006, in Italian
21. A. Fusi, "Utilizzo degli Smart Material nelle vetture di F.1: progetto e sviluppo di un dimostratore tecnologico", Master Thesis, Politecnico di Milano, 2007 (in Italian)